ASM Sci. J.Special Issue 2018(1) AiMS2018, 124-135

Elucidating Mesomorphic and Electrical Properties of Conjugated Acetylide-Imine as Electrochemically Deposited Electron Transporting Materials in Organic Conductive Film

Wan M. Khairul1[1,4*], Y. D. Foong[1], N. M. Sarih[2], O. J. Lee[1], S. K. J. Lim[1], A. I. Daud[1,3] and R. Rahamathullah[1,3]

[1]*School of Fundamental Science, Universiti Malaysia Terengganu, 21030 Kuala Nerus, Terengganu, Malaysia.*

[2] *Department of Chemistry, Faculty of Science, University of Malaya, 50603 Kuala Lumpur, Malaysia*

[3]*Faculty of Engineering Technology, Universiti Malaysia Perlis, Level 1, Block S2, UniCITI Alam Campus, Sungai Chuchuh, Padang Besar,02100, Perlis, Malaysia.*

[4]*Advanced Nano Materials (ANoMa) Research Group, School of Fundamental Science, Universiti Malaysia Terengganu, 21030 Kuala Nerus, Terengganu, Malaysia.*

A new class of liquid crystalline acetylide-imine system was successfully synthesized, characterized and deposited on indium tin oxide (ITO) coated substrate via electrochemical deposition method for potential organic film application. The relationship between liquid crystal molecular structure, phase transition temperature and electrical performance was evaluated. The mesomorphic properties were identified via polarized optic microscopy (POM) which displayed fan-shaped texture of smectic A phase and their corresponding transition enthalpies are in concurrence with DSC and TGA studies. The findings from the conductivity analysis revealed that the fabricated film exhibits good electrical performance where it displayed linear current-voltage relationship of I-V curve. Therefore, this proposed type of molecular framework has given an ideal indication to act as transporting material for application in optoelectronic devices.

Keywords: acetylide-imine, liquid crystal, electrodeposition, electrical studies

I. INTRODUCTION

Almost since its inception, the notion of organic optoelectronics has ignited the imagination towards ultra-lightweight, flexible and large-area devices. Translating imagination into existence has been further fortified when solution-processed emerged as a low-cost and easy-processable thin-film fabrication technique [1]. While a plethora of solution-based deposition techniques have been developed, morphological

*corresponding author:wmkhairul@umt.edu.my

defects remains the biggest technological hurdle mainly due to the structural disorder of molecules on both local (amorphous) and macroscopic (grain boundaries) length scales which limits the charge carrier mobility [1],[2]. This technical drawback is particularly pronounced for electron transporting layer, which attends as the major charge transport carrier in multilayer stack device. In this sense, electrochemical deposition (ECD) is one of the alternative solution-processing route to deposit thin-film with device efficiency complementary to typical solution or vapour deposition [2],[3]-[5]. Into a closer look, ECD can fabricate continuous and ordered thin-film that facilitates intermolecular charge transfer where the thickness of the film can be easily modulated by controlling the amount of charge passes through the electrochemical cell, and a smooth surface morphology of the thin-film is feasible by optimizing the scan rate of cyclic voltammetry [6]. Despite of these morphological advantages offered by ECD, electrodeposition of organic small molecules for use in optoelectronics are still limited to the conventional perylene-based compound [2]. Further synthetic research of novel molecular systems may afford greater understanding of structure-morphology relationships of electrochemical deposited thin-film.

In this contribution, acetylide-imine system has become our subject of interest for liquid crystalline materials as new ECD-processable electron transporting materials as shown in Figure

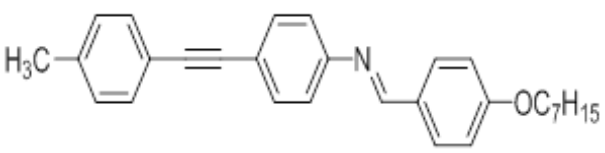

Figure 1. 4-[(4-heptyloxyphenyl)methylene]-4-(phenylethynyl)toluene
(HMPT)

1. Discussing on its structural-property relationship, electrochemically robust and stablility, imine (-HC=N-) moiety is anticipated to transform into new materials with liquid crystalline properties [7]-[8]. In these sense, imine bond (-HC=N-) is incorporated into the molecular structure to increase the length and polarisability anisotropy of the compound core and consequently enhance liquid crystal phase stability [9]. Moreover, imine group is very interesting class of organic compounds in the investigation of their liquid crystal properties from the point of view of their rich polymorphism. By evidence that Schiff Bases undergo electrochemical single-electron-transfer to produce radical imine nitrogen, extension of conjugation has been demonstrated via acetylene functionalization to fine-tune the electrochemical behaviours through resonance stabilization of the electrochemical radical species [10],[7]-[8]. To optimize the communication between electrochemistry and morphology, alkoxy chain has been incorporated not only to manipulate the redox potential shift through its electron donating ability, but also to achieve good solubility that could

assist in the formation of pinhole-free and high-density ECD thin-films [11]-[12]. This electron donating nature of alkoxy function also extended to the photophysics, whereby it could generate electronic push-pull effect with electron deficient Schiff Base π-system to form a unique photochemically active intramolecular charge transfer complex, which is an intriguing feature of electron transporting material [7],[12]. Remarkably, the combination of rigid acetylide-imine core and flexible has afforded the liquid-crystalline property which could self-aligned into an ordered phase at elevated temperature, thus retain the film shape and favor the charge mobility [13]. To integrate all desirable properties into one goal, in this study acetylided-imine were synthesized and fabricated as electrodeposited electron transporting layers, which the current-voltage characteristics and charge transport behaviours were evaluated.

II. MATERIALS AND METHODS

A. Materials and instrumentation

All chemicals and solvents were purchased from standard commercial suppliers namely Sigma Aldrich, Merck, Fisher Scientific and R&M Chemical and were used as received without any special precautions taken during the experimental work-up. The infrared (IR) spectra were recorded on Perkin Elmer 100 Fourier Transform Infrared Spectroscopy in the spectral range of 4000-400 cm^{-1} using potassium bromide (KBr) pellets. The NMR spectra were recorded using Bruker Avance III 400 spectrometer ^{1}H (400.11MHz) and ^{13}C (100.61MHz) by using deuterated chloroform ($CDCl_3$) at room temperature as solvent and internal standard in the range between δ_H 0-15 ppm (^{1}H) and δ_c 0-200 ppm (^{13}C). Thermogravimetric analysis was performed using PerkinElmer TGA Analyzer from 30 °C to 900 °C at a heating rate of 10 °C/min under nitrogen atmosphere. The thermal properties like phase transition temperatures and enthalpy values of liquid crystal mesogens were investigated by modulated DSC Q2000 where the heating and cooling rate at a scanning rate 10 °C/min under nitrogen atmosphere. The liquid crystal phase transitions were investigated by an Olympus polarized light microscope (POM) equipped with Mettler Toledo FP90 hot stage FN82HT. The temperature scanning rate for heating was determined at 10 °C/min while cooling 5 °C/min.

B. Synthesis of 4-Heptyloxybenzaldehyde (1)

The preparation of 1 was accomplished via Williamson ether synthesis through equimolar ratio of heptyl bromide (3.42 g, 19 mmol), 4-hydroxybenzaldehyde (2.32 g, 19 mmol) potassium carbonate (2.63 g, 19 mmol), and KI (1.00 g, 6 mmol) in 70 ml DMF were added into round bottom flask and heated under reflux with con-

stant stirring at 80 °C for overnight (*ca.* 24 hours) afforded a mixture of orange solution and white precipitate of inorganic salt by-product. Once the reaction adjudged completion via thin layer chromatography (TLC), the mixture was allowed to cold to room temperature and filtered to remove inorganic salt by-product. The collected organic phase was extracted using diethyl ether (3 x 100 ml). Later, 5% of NaOH was added into the mixture, extracted with distilled water until the solution reached pH 7. The collected organic phase was then dried over magnesium sulphate, filtered and the solvent was removed *in vacuo* to attain a pale yellowish oil of title compound 1 (3.57 g, 85 %). The synthetic approach applied for 1 is as shown in Scheme 1.

C. Sonogashira Cross-Coupling Reaction: Synthesis of 4[(4-aminophenyl)ethynyltoluene] (2)

Reaction work-up details with respect to the synthesis of 2 following previously reported literature [14]-[15]. 4-iodoaniline (3.00 g, 13.5 mmol) was added into a 250 ml three necks round bottom flask, followed by 5 mmol% CuI and 5 mmol% $Pd(PPh_3)_2Cl_2$. After that, 4-ethynyltoluene (3.18 g, 27 mmol) was added into the mixture, followed by 50 ml of distilled water and 50 ml of triethylamine. Then, the mixture was heated under reflux with a constant stirring at 80 °C for overnight (*ca.* 24 hours) to obtain a two layers mixture. Once the reaction was adjudged completion by thin layer chromatography (TLC), it was allowed to cool to room temperature. Later, the mixture was then filtered, and the collected organic phase was extracted by using DCM (3 x 100 ml). The organic phase was dried over magnesium sulphate and the solvent was removed *in vacuo*. The solid residue was purified over silica gel column chromatography (hexane: CH_2Cl_2; 60: 40) which gave a pale brown solid of title compound 2 (1.63 g, 57 %). The synthetic work for the synthesis of 2 is as shown in Scheme 2.

D. Synthesis of 4-[(4-heptyloxyphenyl)methylene]-4-(phenylethynyl) toluene (HMPT)

The synthesis of HMPT was taken place by adding 2 (0.10 g, 0.48 mmol) into a 250 ml two necks round bottom flask fitted to a dean-stark apparatus, followed by addition of 50 ml of ethanol. Next, the mixture was stirred vigorously until 2 was fully dissolved in ethanol to obtain a brown solution. 4-Heptyloxybenzaldehyde, 1, (0.10 g, 0.48 mmol) in 5 ml ethanol was added dropwise into the round bottom flask. The reaction was continued by stirring the mixture for about 15 minutes before heat was applied. Once the reaction was adjudged completion by TLC, the temperature was increased for distillation to take place and to remove excess ethanol from the round bottom

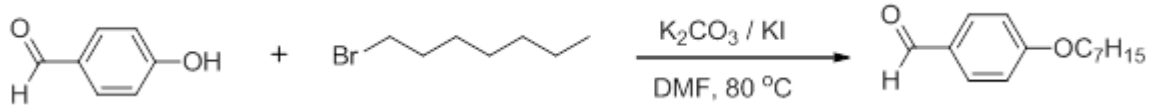

Scheme 1. Synthetic approach for the synthesis of 4-heptyloxybenzaldehyde (1)

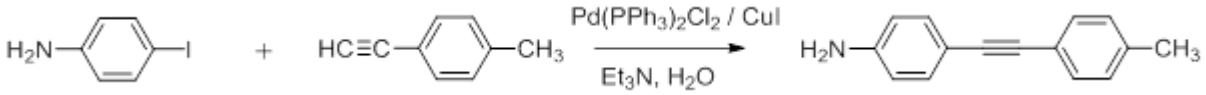

Scheme 2. Synthetic approach for the synthesis of 4[(4-aminophenyl)ethynyltoluene] (2)

flask (*ca.* 20 ml). After that, the mixture was cooled to room temperature. The crystallization was induced when the mixture was added into ice-bath to obtain pale yellow solid precipitate. The obtained precipitated was then filtered, recrystallized over hot acetonitrile to attain a pale-yellow solid of 3 (0.17 g, 86 %). The synthetic pathway of 3 is as shown in Scheme 3.

E. Fabrication of Organic Thin Film

The thin films were prepared by using electrochemistry method via Electrochemical Impedance Spectroscopy (EIS) in the following conditions: 0.05 V, 0.05 V/S, and potential range -3 V until 3 V in tetrahydrofuran (THF). Figure 2 shows the general illustration arrangement of HMPT/ITO.

F. Electrical Characteristic Study

HMPT/ITO thin film was prepared by using electrochemistry method and these thin films were investigated on their performance by plotting I-V curve to investigate the potential and tendency to be applied as an active layer organic thin film transistor. I-V curve was plotted by using Four Point Probe system consist of the Jandel Universal Probe combined with a Jandel RM3 Test Unit. In this study, the forward voltage and reverse voltage were measured by setting the current as manipulation variable so that by changing the current, the voltage can be measured. Two outer probes supply a voltage difference that drives a current through the film. Meanwhile the two-inner probe pick up a voltage difference and the forward voltage and reverse voltage were recorded.

III. RESULTS AND DISCUSSIONS

A. Infrared (IR) Spectroscopy Analysis

Infrared spectrum of HMPT revealed all the expected bands of interest namely ν(C-H aromatic), ν(CH aliphatic), ν(C≡C), ν(C-O), ν(C=N). The broad IR band at 3447 cm^{-1} was assigned as stretching vibrations of v(C-H aromatic) in the phenyl ring. The band was shifted to a higher wavelength with increasing band broadness compared to its precursor due to the effect of charge resonance in regularly stacked of

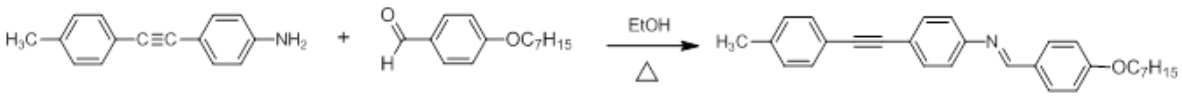

Scheme 3. Synthetic approach for the synthesis of 4-[(4-heptyloxyphenyl)methylene]-4-(phenylethynyl) toluene (HMPT)

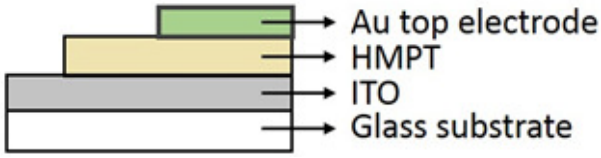

Figure 2. The general illustration of HMPT/ITO layers

multiple aromatic groups. The absorption bands of ν(C-H aliphatic) and ν(C-O) were observed respectively in the range of 2922 cm^{-1} to 2858 cm^{-1} and 1169 cm^{-1} [16]. The assignments of these stretching modes were made by comparing to their precursor and shifting wavenumbers were associated with the conjugation effect as HMPT has relatively greater extent of conjugation as compared to its precursor. The ν(C≡C) of the tolane moiety occurred at 2212 cm^{-1} as weak intensity peak where a diminished absorption intensity of ν(C≡C) was observed due to the effect of the inter-stacking interaction and dipole moment of the molecule [17]-[18]. Additionally, the presence of ν(C=N) stretching vibration can be observed at 1621 cm^{-1} in which it is highly indicated to the imine formation and molecular structure of HMPT [19]-[20]. The ν(C=N) can be noticed at a low frequency due to the conjugation of π-electrons caused by the effect of tolane and para-substituted phenyl ring along with delocalization of nitrogen pair into imine double bond that eventually lowered the ν(C=N) wavenumber [21].

B. ^{1}H and ^{13}C Nuclear Magnetic Resonance (NMR) Analysis

The ^{1}H NMR spectrum for HMPT showed methyl resonance at δ_H 0.90 ppm while protons for the alkoxy group were observed in the range of δ_H 1.30-1.83 ppm. For R-O-CH_2, the signal was detected at δ_H 4.02 ppm due to the contribution of electronegativity of the oxygen atom. Meanwhile, the aromatic protons of the para-substituted aromatic rings can be clearly observed as pseudo-doublet resonances in the range of δ_H 6.98-7.85 ppm. In addition, azomethine proton (NH) was observed as a singlet at downfield, δ_H 8.38 ppm. The disappearance of amine and aldehyde protons that accompanied with the appearance of azomethine proton confirming that the amine was reacted with aldehyde to produce imine moiety [22]. The ^{13}C NMR data of HMPT was consistent with the proposed molecular structure. The methyl resonance can be clearly observed at δ_c 14.09 ppm and carbon resonances for alkyl were detected in the range of δ_c 21.53-31.78 ppm, which revealed a good agreement with the previous re-

ports on the similar systems. Whilst, the chemical shift for R-CH_2-O- can be found at δ_c 68.25 ppm due to the deshielding effect in the presence of oxygen atom. Meanwhile, the acetylide carbons of the tolane moieties can be clearly observed as two resonances at δ_c 88.82 ppm and δ_c 89.73 ppm where the splitting is due to the influence of their non-symmetrical structure, which revealed a good agreement with the previous reports on the similar systems [15]. In addition, aromatic carbon resonances were also observed in the range of δ_c 114.75-160.00 ppm which attributed to their para-substituted aromatic systems. The resonance of C=N was observed at δ_c 162.10 ppm.

C. Thermal, Mesogenic and Microstructure Studies

Thermal stability of HMPT was investigated via thermogravimetric (TGA) and differential scanning calorimetry (DSC) analysis. The molecule is stable up to 300 °C and the degradation process showed two stages of major mass loss as depicted in Figure 3a. The initial degradation took place at around 305 °C (T_{onset}) and ended at around 390 °C (T_{offset}) with maximum degradation (T_{max}) of 360 °C. Meanwhile, second stage started to degrade at 415 °C (T_{onset}) and ended at 505 °C (T_{offset}) with maximum degradation (T_{max}) of 450 °C. During the decomposition of these stages, the total mass loss was about 75%. Generally, this thermal behaviour are in agreement with the previously reported related compounds [14]. Considering T_d is above its LC phase transition temperature, HMPT could maintain good thermal and morphological stabilities when thermally annealed at its LC phase transition temperature to allow *in-situ* self-organization during the device fabrication step.

On the other hands, the POM studies of HMPT imply nematic phase reflected the marbled texture upon heating between 80-130 °C (Figure 4) before clearing to the isotropic liquid at 270 °C. The material was cooled from the clearing at 10°C per minute to 132-122 °C, where the formation of a fan-shaped texture occurred and assigned as a smectic A phase. Upon further cooling to 80 °C a transition occurs which leading to a nematic phase identified by its characteristic of marbled texture as depicted in Figure 5. In this present case, the combination of C≡C bond and a flexible tail suggests that HMPT exhibited liquid crystalline phases at elevated temperatures [23]-[24]. Additionally, the imine (CH=N) linking group is one of the factors influencing the target compound exhibit nematic phase as expected since this ligand has long molecular lengths coupled with extension of the conjugation through aromatic rings. DSC analysis is concurrence with POM studies. During heating mode two anomalies are visible, which correspond to the phase transitions. At 80°C, the transition from the crystal phase to nematic phase takes place. Next, the peak at about 130

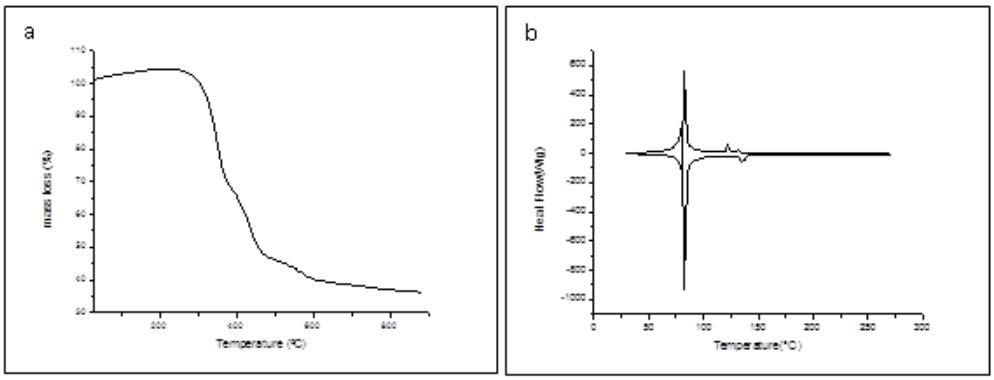

Figure 3. (a) TGA and (b) DSC thermograms of HMPT

°C corresponds to the transition nematic phase. Then, upon cooling, there are three anomalies are presence which showed isotropic → smectic A transition temperature (T_L → SmA) at 132°C and 122°C, yet the transition smectic → Anematic transition is present on the relevant diagram at 80°C as shown in Figure 3.

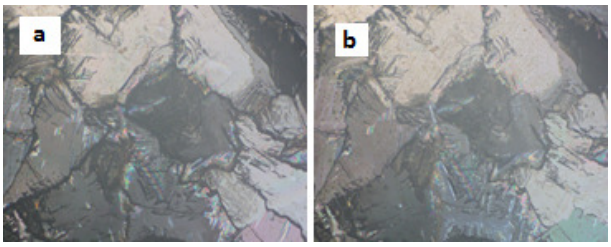

Figure 4. (a) and (b): Marble texture of Nematic phase at 80°C and 130°C on heating

Figure 5. (a) fan-shaped texture of smectic A phase at 132°C ; (b) fan-shaped texture of smectic A phase at and 122°C ; (c) Marble texture of Nematic phase at 80°C on cooling

Considering the molecular assembly of π-conjugated aromatic molecules is largely dominated by the π-π interaction between the planar π-system (in cooperation with the hydrophobic interactions between the alkoxy chains), HMPT is anticipated to produce similar intermolecular arrangement and therefore approximately the same morphology of the final assembled materials as indeed disclosed by the SEM imaging displayed in Figure 6. The amphiphilic property of HMPT is highly favourable for self-assembly through π-π stacking in hydrophilic solvent, where the hydrophilic Schiff base core tends to stretch out into the solvent, while the hydrophobic alkoxy chains tend to interdigitate to hold the HMPT scaffolds, hence facilitating the π-π stacking growth [13]. In short, based on the SEM analyses, HMPT can be readily assembled into well-structured that promise in fabricating well-ordered thin film.

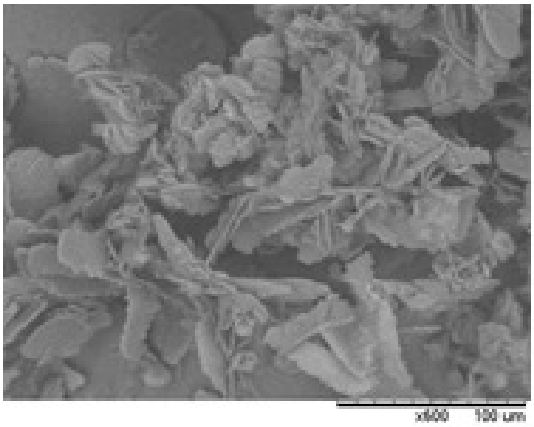

Figure 6. SEM images of HMPT material

D. Electrical Conductivity Studies

The electrical conductivity (EC) study of HMPT thin film in the Au/HMPT/ITO metal-organic conductive layer-metal oxide configuration was evaluated by using Four Point Probe. The EC of the thin film was measured based on the voltage values, while the current was set as constant. The current value was applied only from the range of 1 mA to 10 mA due to limitation of the available instrumentation. Both forward biased voltage and reverse biased voltage were recorded and the I-V curve was plotted as depicted in Figure 7 (left). From the data analysis, I-V curves measurement displayed ohmic current-voltage relationship where the electrical conductivity of HMPT increased proportional with the applied voltage. The asymmetry of I-V curve is caused by the different top and bottom electrodes work functions, ϕ for ITO layer and Au electrode of 4.8 eV and 5.1 eV, respectively at the electrode-film interface. The schematic diagram of an energy band for Au/HMPT/ITO configuration is depicted in Figure 7 (right) with the energy band gap of HMPT (3.61 eV) calculated from density functional theory. In short, the preliminary study of electrical conductivity of HMPT showed positive and satisfactory results for this material to be applied as conductive film due to its properties, in which the system possesses fair conjugation in the molecular framework.

IV. SUMMARY

In conclusion, the role and performance of new liquid crystalline semiconductor material of acetylide-imine has been successfully synthesized and eventually deposited on ITO substrate via simple electrochemical deposition method. This material possesses thermal stability at high temperature and displayed fan-shaped smectic A during the cooling processes. The fabricated films also exhibited good electrical performance under various current values. Thus, the results revealed that this liquid crystalline material can be employed as ECD-transporting material in conductive film application.

V. ACKNOWLEDGMENT

The authors would like to express gratitude to the Ministry of Higher Education (MOHE) for research grant (FRGS59366), MyBrain Fund for postgraduate students scholarship, Department of Chemistry University of Malaya, School

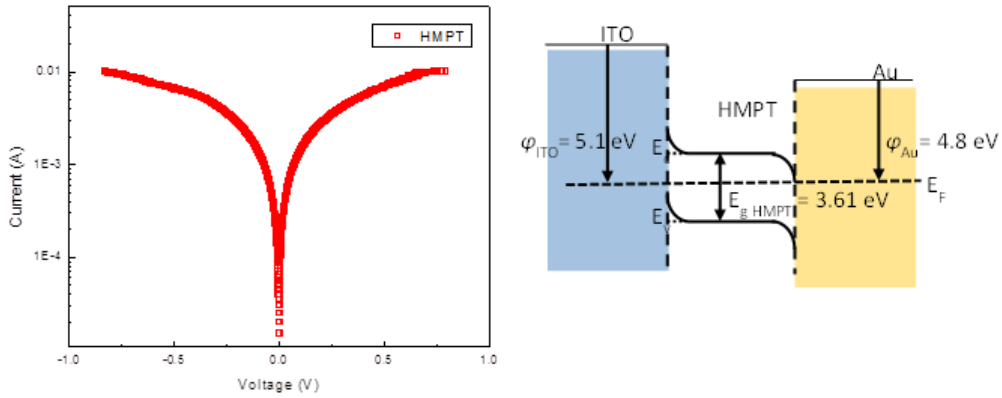

Figure 7. IV curve (left) and energy band schematic diagram (right) of Au/HMPT/ITO configuration.

of Fundamental Science, School of Ocean Engineering and Institute of Marine Biotechnology (IMB) Universiti Malaysia Terengganu for facilities and research aids.

[1] Diao, Y, Shaw, L, Bao, Z, Mannsfeld, SC, 2014, Morphology control strategies for solution-processed organic semiconductor thin films, *Energy Environ.* Sci., vol. 7, pp. 2145-2159.

[2] Allwright, E, Berg, DM, Djemour, R, Steichen, M, Dale, PJ, Robertson, N, 2014, Electrochemical deposition as a unique solution processing method for insoluble organic optoelectronic materials, *J. Mater. Chem. C.*, vol. 2, pp. 7232-7238.

[3] Allwright, E, Silber, G, Crain, J, Matsushita, MM, Awaga, K, Robertson, N, 2016, Electrochemical deposition of highly-conducting metal dithiolene films, *Dalton Trans.*, vol. 45, pp. 9363-9368

[4] Dalgleish, S, Awaga, K, Robertson, N, 2011, Formation of stable neutral copper bisdithiolene thin films by potentiostatic electrodeposition, *ChemComm.*, vol. 47, pp. 7089-7091.

[5] Rahamathullah, R, Khairul, WM, 2017, Evaluation on the electrochemically deposited alkoxy thiourea as liquid crystalline semiconductor film, *Appl. Surf. Sci.*, vol. 424, pp. 45-51.

[6] Yu, T, Xu, J, Liu, L, Ren, Z, Yang, W, Yan, S, Ma, Y, 2016, Electrochemically deposited interlayer between PEDOT: PSS and phosphorescent emitting layer for multilayer solution-processed phosphorescent OLEDs, *J. Mater. Chem. C.*, vol. 4, pp. 9509-9515.

[7] Bolduc, A, Mallet, C, Skene, W, 2013, Survey of recent advances of in the field of -conjugated heterocyclic azomethines as materials with tuneable properties. *Sci. China Chem.*, vol. 56, pp. 3-23.

[8] Sultan, Y, Selehattin, Y, Gulsen, S, Murat, S, Mustafa, Y, Kamran, P, 2013, synthesis, spectroscopic studies and electrochemical properties of Schiff bases derived from 2-hydroxyaldehydes and phenazopyridine hydrochloride. *J. Serb. Chem. Soc.*, vol. 78, pp. 795-804

[9] Iwan, A, 2010, Thermotropic and opto (electrical) properties of liquid crystalline imine with two fluorinated chains. *J. Mol. Liq.*, vol. 157, pp. 67-72.

[10] Zhao, YP, Wu, LZ, Si, G, Liu, Y, Xue, H, Zhang, LP, Tung, CH, 2007a, Synthesis, spectroscopic, electrochemical and Pb2+-binding studies of tetrathiafulvalene acetylene derivatives, *J. Org. Chem.*, vol. 72, pp. 3632-3639.

[11] You, JD, Tseng, SR, Meng, HF, Yen, FW, Lin, IF, Horng, SF, 2009, All-solution-processed blue small molecular organic light-emitting diodes with multilayer device structure. Org. *Electron*, vol. 10, pp. 1610-1614.

[12] Zhao, C, Zhang, Y, Li, R, Li, X, Jiang, J, 2007b, Di (alkoxy)-and di (alkylthio)-substituted perylene-3,4;9,10-tetracarboxy diimides with tunable electrochemical and photophysical properties, *J. Org. Chem.*, vol. 72, pp. 2402-2410.

[13] Iino, H, Usui, T, Hanna, JI, 2015, Liquid crystals for organic thin-film transistors, *Nat. Commun.*, vol. 6, pp. 6828.

[14] Khairul, WM, Daud, AI, Hanifaah, NAM, Arshad, S, Razak, IA, Zuki, HM, Erben, MF, 2017, Structural study of a novel acetylide-thiourea derivative and its evaluation as a detector of benzene. *J. Mol. Struct.*, vol. 1139, pp. 353-361.

[15] Daud, AI, Khairul, WM, Zuki, HM, Kubulat, K, 2015, Aerobic synthetic approach and characterisation of some acetylidethiourea derivatives for the detection of carbon monoxide (CO) gas. *J. Mol. Struct.* vol. 1093, pp.172-178.

[16] Abdul-Kadir, M, Philip, RC, Hanton, LR, Courtney, AH, Sumby, CJ, 2012, Pre-organisation of a hydrogen bonding mismatch: silver(I) diamide ligand coordination polymers versus discrete metallo-macrocyclic assemblies, *Supramolecular Chemistry*, vol. 24(8), pp. 627-640.

[17] Ishida, T, Shibata, M, Fujii, K, Inoue, M, 1983, Inter-and intramolecular stacking interaction between indole and adeninium rings, *Biochem.*, vol. 22, pp. 3571-3581.

[18] Martinez, CR, Iverson, BL, 2012, Rethinking the term pi-stacking, *Chem. Sci.*, vol. 3, pp. 2191-2201

[19] Dubey, R, Yerrasani, R, Karunakar, M, Singh, AK, Gupta, R, Ganesan, V, Rao, TR, 2017, Benzimidazole based mesogenic Schiff-bases: Synthesis and characterization, *J. Mol. Liq.*, vol. 240, pp. 106-114

[20] Gupta, BD, Datta, C, Das, G, Bhattacharjee, CR, 2014, Rod shaped oxovanadium (IV) Schiff base complexes: Synthesis, mesomorphism and influence of flexible alkoxy chain lengths. *J. Mol. Struct.*, vol. 1067, pp. 177-183.

[21] Sek, D, Grucela-Zajac, M, Krompiec, Janeczek, H, Schab-Balcerzak, E, 2012, New glass forming triarylamine based azomethines as a hole transport materials: Thermal, optical and electrochemical properties. *Opt. Mater.* vol. 34, pp. 1333-1346.

[22] Moorthy, NHN, Vittal, UB, Karthikeyan, C, Thangapandian, V, Venkadachallam, AP, Trivedi, P, 2017, Synthesis, antifungal evaluation and in silico study of novel Schiff bases derived from 4-amino-5 (3, 5-dimethoxy-phenyl)-4H-1, 2, 4-triazol-3-thiol. *Arabian J. Chem.*, vol. 10, pp. S3239-S3244.

[23] Sepelj, M, Lesac, A, Baumeister, U, Diele, S, Nguyen, HL, Bruce, DW, 2007, Intercalated liquid-crystalline phases formed by symmetric dimers with an , -diiminoalkylene spacer. J.

Mater. Chem., vol. 17, pp. 1154-1165

[24] Ha, ST, Ng, MY, Subramaniam, RT, Ito, MM, Saito, A, Watanabe, M, Lee, SL, Bonde, NL, 2010, Mesogenic azomethine esters with different end groups: Synthesis and thermotropic properties, Inter. *J. Phys. Sci.*, vol. 5, pp. 1256-1262